Acta Neuropathologica (2022) 143:531–545
https://doi.org/10.1007/s00401-022-02416-5

ORIGINAL PAPER

Patterns of amygdala region pathology in LATE-NC: subtypes that differ with regard to TDP-43 histopathology, genetic risk factors, and comorbid pathologies

Matthew D. Cykowski[1,2] · Anithachristy S. Arumanayagam[1] · Suzanne Z. Powell[1] · Andreana L. Rivera[1] · Erin L. Abner[3,4] · Gustavo C. Roman[2,5] · Joseph C. Masdeu[2,5] · Peter T. Nelson[3,6]

Received: 1 November 2021 / Revised: 25 March 2022 / Accepted: 26 March 2022 / Published online: 2 April 2022

Abstract

Transactive response (TAR) DNA-binding protein 43 kDa (TDP-43) pathology is a hallmark of limbic-predominant age-related TDP-43 encephalopathy (LATE). The amygdala is affected early in the evolution of LATE neuropathologic change (LATE-NC), and heterogeneity of LATE-NC in amygdala has previously been observed. However, much remains to be learned about how LATE-NC originates and progresses in the brain. To address this, we assessed TDP-43 and other pathologies in the amygdala region of 184 autopsied subjects (median age = 85 years), blinded to clinical diagnoses, other neuropathologic diagnoses, and risk genotype information. As previously described, LATE-NC was associated with older age at death, cognitive impairment, and the *TMEM106B* risk allele. Pathologically, LATE-NC was associated with comorbid hippocampal sclerosis (HS), myelin loss, and vascular disease in white matter (WM). Unbiased hierarchical clustering of TDP-43 inclusion morphologies revealed discernable subtypes of LATE-NC with distinct clinical, genetic, and pathologic associations. The most common patterns were: Pattern 1, with lamina II TDP-43 + processes and preinclusion pathology in cortices of the amygdala region, and frequent LATE-NC Stage 3 with HS; Pattern 2, previously described as type-β, with neurofibrillary tangle-like TDP-43 neuronal cytoplasmic inclusions (NCIs), high Alzheimer's disease neuropathologic change (ADNC), frequent *APOE* ε4, and usually LATE-NC Stage 2; Pattern 3, with round NCIs and thick neurites in amygdala, younger age at death, and often comorbid Lewy body disease; and Pattern 4 (the most common pattern), with tortuous TDP-43 processes in subpial and WM regions, low ADNC, rare HS, and lower dementia probability. TDP-43 pathology with features of patterns 1 and 2 were often comorbid in the same brains. Early and mild TDP-43 pathology was often best described to be localized in the "amygdala region" rather than the amygdala proper. There were also important shared attributes across patterns. For example, all four patterns were associated with the *TMEM106B* risk allele. Each pattern also demonstrated the potential to progress to higher LATE-NC stages with confluent anatomical and pathological patterns, and to contribute to dementia. Although LATE-NC showed distinct patterns of initiation in amygdala region, there was also apparent shared genetic risk and convergent pathways of clinico-pathological evolution.

Keywords *GRN* · PART · Neuropathology · Tauopathy · Preclinical · Nondemented · DLB · Lewy

✉ Matthew D. Cykowski
mdcykowski@houstonmethodist.org

[1] Department of Pathology and Genomic Medicine, Houston Methodist Hospital, Houston, TX 77030, USA

[2] Methodist Neurological Institute Department of Neurology, Houston Methodist Hospital, Weil Cornell Medicine, Houston, TX 77030, USA

[3] Sanders-Brown Center On Aging, University of Kentucky, University of Kentucky, Lexington, KY 40536, USA

[4] Department of Epidemiology, University of Kentucky, Lexington, KY 40536, USA

[5] Nantz National Alzheimer Center, Houston Methodist Hospital, Houston, TX 77030, USA

[6] Department of Pathology, University of Kentucky, Lexington, KY 40536, USA

Introduction

The amygdala region comprises an anatomically heterogeneous set of brain structures that normally play a role in cognitive function, emotional processing, integration of olfactory input, and autonomic responses [2, 33, 54]. Consistent with its many functional roles, this brain region is anatomically complex [48]. The amygdala region consists of the corticomedial and basolateral subdivisions of the amygdala itself (the "amygdala proper") [54], the temporal horn of the lateral ventricle and adjacent white matter and vasculature, the ventrolateral extension of the basal forebrain [15], the ventral extensions of putamen and claustrum, periallocortex (transentorhinal and entorhinal cortex), and neocortical regions of the inferior temporal lobe that are lateral to the collateral sulcus [7, 9, 35].

The amygdala region appears particularly susceptible to neurodegenerative disease pathology [40]. This brain area is implicated in early-stage tau, α-synuclein, and TAR DNA-binding protein 43 kDa (TDP-43) proteinopathies [9, 14, 31, 40]. TDP-43 pathology is one of the most common age-related pathologies [6, 23, 24, 27], initially described in patients with frontotemporal lobar degeneration (FTLD) and amyotrophic lateral sclerosis (ALS) [12, 34, 44], and thereafter recognized in other diseases [3, 5, 6, 11, 29, 51]. TDP-43 pathology can be observed in a presumed preclinical phase, but overall this pathologic biomarker is strongly associated with cognitive impairment independent of comorbid pathologies (e.g., Alzheimer's disease-associated neuropathology, or ADNC) [29, 41, 53]. To aid in the recognition and classification of TDP-43 pathology in aging, a 2019 consensus working group proposed the term "limbic-predominant age-related TDP-43 encephalopathy", or LATE [42].

The amygdala has been reported to be the earliest anatomic location of TDP-43 pathology in aging (LATE-NC Stage 1) [28, 39, 42]. In ground-breaking work, Josephs and colleagues described two patterns of TDP-43 proteinopathy in the amygdala, terming those patterns "type-β", for fibrillary TDP-43 pathology associated with neurofibrillary tangles, and "type α", for typical TDP-43 pathology in the form of neuronal inclusions and/or neurites [27]. Following these studies, important questions remain with respect to LATE neuropathologic change (LATE-NC) in amygdala and surrounding structures. Do the patterns of TDP-43 pathology overlap in individual brains? Are there other TDP-43 pathologic patterns, and if so, how do these patterns relate to comorbid pathologies and genetic risk factors? Does TDP-43 pathology in the amygdala begin in a predictable anatomic focus in all patients? Does LATE-NC ever begin outside of the amygdala per se (i.e., is it ever present in adjacent brain regions, but not in "amygdala proper")? Does the involvement of the amygdala region at higher stages of LATE show convergence of TDP-43 pathology? Conversely, are there structures within the amygdala region more resistant to TDP-43 pathology even as pathologic burden increases? And finally, do all patterns of LATE-NC eventually result in higher-stage LATE-NC and dementia?

The aim of the current study was to enhance our understanding of LATE-NC heterogeneity, and to elucidate how TDP-43 pathologic patterns are associated with genetics, clinical disease severity, and comorbid pathologies. Pathologic features in the amygdala region were graded blind with respect to clinical diagnoses, genetic risk factors, and comorbid pathologies, and all included brains were assigned to TDP-43 pathologic pattern subtypes that were generated using an unbiased clustering algorithm. These patterns were then correlated with other parameters. Our findings build on prior studies about how TDP-43 pathology in LATE-NC originates and evolves in the aging brain.

Materials and methods

Case identification

Samples and data evaluated were from autopsy study participants from two different institutions: Houston Methodist Hospital (HMH, in Houston, Texas, USA) and the University of Kentucky Alzheimer's Disease Research Center at Sanders-Brown Center on Aging (UKY [47], in Lexington, Kentucky, USA) (see Supplemental Table 1 (online resource)). Study participants were along a continuum from normal cognition to severe amnestic dementia. This was a convenience sample and there were no specific age cutoffs, but the demographics reflect the characteristics of the participants at each of the institutions. Research consent was provided for all study participants by the patients (and/or caregivers), or the next-of-kin at the time of autopsy consent, per the guidelines of each institution. The study was performed with the approval of the Institutional Review Boards at HMH and UKY.

Exclusion criteria

Samples were excluded from participants with diagnoses of amyotrophic lateral sclerosis, clinical frontotemporal dementia with FTLD-TDP, FTLD-tau and other rare tauopathies (progressive supranuclear palsy, corticobasal degeneration), or other rare neurological diseases (e.g., prion disease). Samples were also excluded if review of anatomic sections showed poor orientation, incomplete sampling of the region, or acute hypoxic/ischemic injury.

Histologic preparations and immunostaining

For evaluation of pathologic features in the amygdala region, formalin-fixed paraffin-embedded (FFPE) tissue blocks were sectioned at 6 µm, mounted on charged slides, and dried overnight at 60 °C. Serial sections were stained for hematoxylin and eosin (H&E) and cresyl violet/ luxol fast blue (LFB), using a previously described modified Klüver–Barrera protocol [40]. All including subjects and slides had appropriate amygdala region orientation, available clinical information, and whole-brain autopsy diagnoses.

All samples were stained for TDP-43 using phosphorylation-dependent (hereafter, "pTDP IHC") and non-phosphorylation-dependent antibodies (hereafter, "TDP-43 IHC"), and were also stained for phospho-tau (AT8). The immunostaining procedure used has previously been described in detail [16, 22] and details are provided in the Supplemental Methods (online resource). Both TDP-43 antibodies were used as many laboratories with large brain banks rely on pTDP-43 IHC to detect TDP-43 proteinopathies [30] and TDP-43 IHC may be particularly sensitive to granular pre-inclusions [10, 13, 17], including in amygdala region [18].

Amygdala region regions-of-interest

The regions-of-interest (ROIs) examined here are shown in Fig. 1, Supplemental Figs. 1 and 2 (online resource). ROIs included occipitotemporal cortex (*OTCtx*), transentorhinal and entorhinal cortex (*TECtx/ECtx*), corticomedial amygdala (*CM*), basolateral amygdala (*BL*), lateral subdivision of the lateral nucleus (*La-L*), and white matter (*WM*). Structures that were not consistently present across samples included the centromedial nuclear group—a dorsally located nuclear group in amygdala, the basal forebrain with magnocellular neurons of the nucleus basalis, the ventral extension of claustrum and putamen, and anterior hippocampus. However, pTDP and TDP-43 IHC pathologic observations were recorded when these structures were present.

The ROIs were defined as follows using H&E and LFB/Nissl-stained sections (Supplemental Fig. 1, online resource, which shows example study material). *OTCtx* was defined as neocortex of fusiform gyrus lateral to the collateral sulcus [7, 20, 27, 35]. *TECtx* and *ECtx* were defined here as used previously [9]. No attempt was made to separate *TECtx* and *ECtx* into two ROIs since large multipolar neurons in the pre-α layer of *ECtx* intercalate with laminae III and IV of *TECtx* [7]. The *CM* amygdala ROI included several fields in and around the uncus, including the subpial zone and molecular layer overlying amygdala, the underlying ventral cortical nucleus of amygdala containing several layers of pyramidal neurons [4], and the transition zone between ECtx and amygdala at the uncus, also known as the parahippocampal–amygdaloid transition area (PHA) [35]. *BL* amygdala represented the largest study ROI (Supplemental Figs. 1, 2, online resource), comprising large neurons of lateral, basal and accessory basal subnuclei, and scattered islands of small neurons ("intercalated nuclei") [54]. *La-L* amygdala was the lateral-most ROI, very distinct as stripes of gray matter with medium-sized and large neurons and intervening white matter. The *WM* ROI focused on the white matter positioned between amygdala and entorhinal cortex. This *WM* ROI includes perivascular and periventricular white matter, enriched in corpora amylacea, veins with thickened and fibrotic walls ("venous collagenosis"), and rarefied white

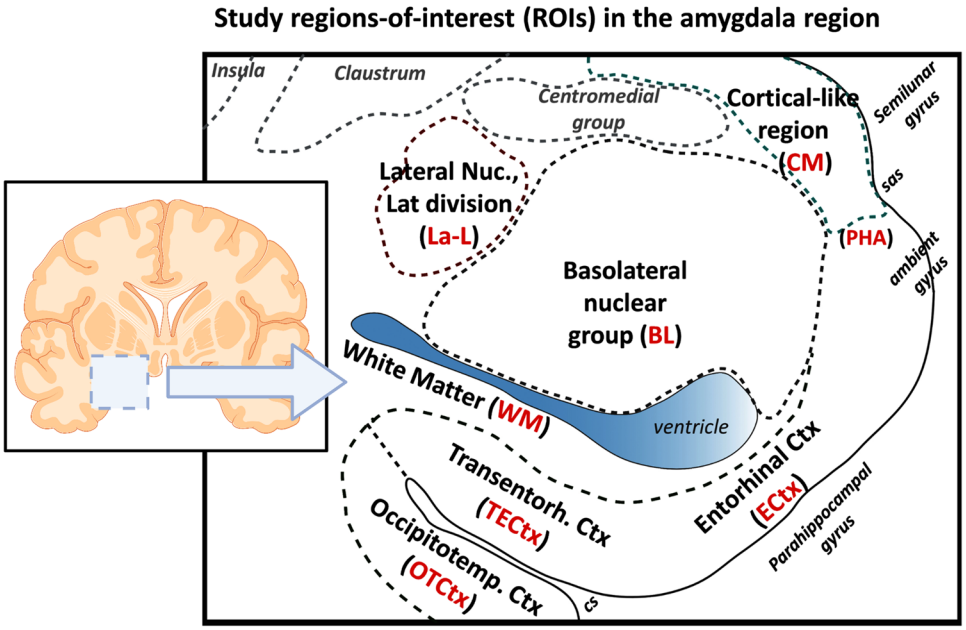

Fig. 1 Regions-of-interest (ROIs) in the amygdala region. A schematic of the amygdala region and the associated ROIs is shown, with parahippocampal gyrus, collateral sulcus (cs) and semiannular sulcus (sas) labeled for reference. Study ROIs are in red, bolded font. Although not study ROIs, insula, ventral claustrum, centromedial nuclear group, and basal forebrain components were assessed for pTDP-43 pathology in all cases when present. Schematic created with BioRender

matter on LFB stain (Supplemental Fig. 3, online resource). This area, also referred to as "subamygdaloid white matter" [54], contains fiber bundles passing between the amygdala, entorhinal cortex, posterior parahippocampal gyrus, and hippocampus.

Assessment of TDP-43 and pTDP-43 pathologies

TDP-43 IHC and pTDP IHC pathologies were scored blinded to clinical and pathologic data. Cases designated as "Positive" had inclusions in the same ROI by both TDP-43 and pTDP IHC. In addition, 6 morphologic subtypes of TDP-43 and pTDP IHC pathology were recorded for each participant as being present or absent. The 6 recorded morphologies were as follows:

(1) neurofibrillary tangle (NFT)-like neuronal cytoplasmic inclusions, consistent with type-β NCIs as previously described [27]; (2) round NCIs in amygdala; (3) small NCIs with non-tapering neurites in lamina II of cortex (FTLD-like); (4) granular preinclusions; (5) thick neurites in amygdala; and (6) tortuous processes in the subpial region of the CM ROI and the WM ROI. The typical appearance and location of each of these 6 key morphologies is shown in Fig. 2.

For each case, semiquantitative measures were applied to determine the severity of pTDP-43 pathology across the entire amygdala region and pTDP-43 pathologic burden within each ROI. The four-tiered semiquantitative scoring approach using pTDP-43 IHC is shown in Supplemental Fig. 4 (online resource). Briefly, each amygdala sample was scored for pTDP-43 pathology as very mild pathology in 1 ROI (Score 1), multifocal and mild pathology in ≥ 2 ROIs (Score 2), multifocal and moderate pTDP-43 pathology (Score 3), and severe and extensive pathology (Score 4). For each ROI, pTDP-43 inclusion density was recorded in a representative 400 × field, recording 0–30 inclusions per 400 × field (maximum value was 30, as it is difficult to enumerate individual inclusions beyond that). We have previously demonstrated that TDP-43 IHC inclusion density assessed this way is strongly correlated with image-based analyses of pTDP IHC [13].

Assessment of Tau pathologies

Phospho-tau (AT8) immunostaining was used to assess argyrophilic grain pathology [8, 26] and aging-related tau astrogliopathy (ARTAG) [31, 32], using standard criteria. ARTAG was recorded as being subpial, white matter and/or gray matter in location. NFT pathology was assessed and was concordant with ADNC pathology levels in all samples (these data were analyzed after blinded pathologic evaluations).

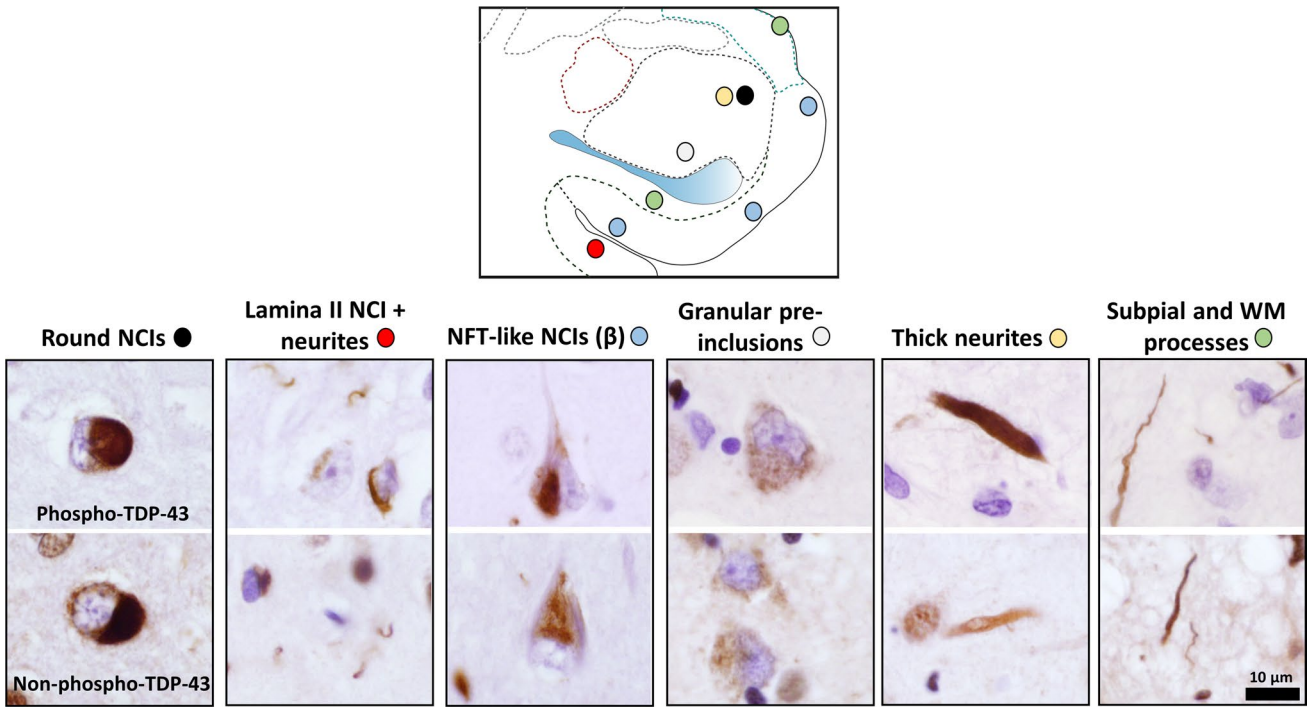

Fig. 2 Key TDP-43 inclusion morphologies in LATE-NC. Six key TDP-43 inclusion morphologies are shown, with paired pTDP (top row) and TDP-43 IHC (bottom row). As shown, both pTDP and TDP-43 IHC can identify these pathologies. The colored circles adjacent to the morphology labels are placed on the Fig. 1 schematic to indicate their most common anatomic position in the amygdala region

Additional amygdala pathologies

Blinded to pTDP and TDP IHC data, H&E and LFB/Nissl stains were used to assess neuronal loss, vascular pathology, reactive astrocytosis, and myelin loss in the amygdala region, using FFPE sections obtained serially adjacent to those used for Tau, TDP-43, and pTDP IHC studies. The grading scheme for each of these pathologies is shown in Supplemental Fig. 5 (online resource). A four-tiered scale was also used to rate small vessel arteriolosclerosis in the section as being absent, mild, moderate, or severe. Vascular pathology with rarefaction in subamygdaloid WM was rated as present (see example in Supplemental Fig. 3, online resource) or absent.

Immunofluorescence studies

The immunofluorescence protocol used has been described in detail previously [16, 22] and is described in the Supplemental Methods (online resource). Briefly, a convenience sample of cases with TDP-43, pTDP, and tau pathology were selected for further examination using double immunofluorescence labeling. Cases were selected with prominent NFT-like (type-β) pTDP-43 NCIs, lamina II TDP-43 pathology, and subpial and WM pTDP-43 + processes. Double labeling was performed for Tau and non-phosphorylated TDP-43. Selected samples with prominent pTDP-43-positive processes were examined using double labeling with the axonal markers MAP-2, tubulin, and a pan-neuronal marker, as well as GFAP and CD44.

Single nucleotide polymorphisms (SNP) genotyping

For SNP genotyping, DNA was isolated from FFPE samples using the QIAamp DSP DNA FFPE Tissue kit (Qiagen, catalogue ID 60,404, Germany) following manufacturer instructions. SNP genotyping was performed using TaqMan™ probes for *APOE* rs429358/ rs7412, *ABCC9* rs704180, *GRN* rs5848, *KCNMB2* rs12496790, and *TMEM106B* rs1990622 (Thermo Fisher Scientific, USA) on a Bio-Rad CFX 96 Real-Time System (Bio-Rad, USA). Interpretation was performed using the Allelic Discrimination function in CFX Maestro Software (Bio-Rad, USA). Further details of SNP genotyping are provided in the Supplemental Methods file (online resource).

Clinical information and additional neuropathologic data

After pathologic data and genotyping were completed, additional clinical and pathologic data were added to the study database. Demographic and clinical data included participant age at death, sex, and cognitive status (normal, mild cognitive impairment, or dementia) proximal to death. Pathologic measures included brain weight, ADNC level (NIA/AA 2012) ("High", "Intermediate", "Low", "Not") [37], presence or absence of hippocampal sclerosis (HS), Lewy body disease (transitional/neocortical versus amygdala limited), presence or absence of primary age-related tauopathy (PART) [14], whole-brain arteriosclerosis (on a four-tied scale), Thal Aß phase [50], Braak NFT stage [9], and CERAD plaque frequency rating [36].

Statistical analyses

Two-sided Wilcoxon ranked-sum tests and Chi-square (χ^2) testing, as implemented in the software program R [49], were performed to examine group differences and associations of LATE-NC pathology versus the control group. The association between risk alleles and TPD-43 status was examined using the 'epitools' package in R [49]. The normal approximation (Wald) with small sample adjustment was used to determine odds ratio (OR) and confidence intervals. The publicly available tool Morpheus (https://software.broadinstitute.org/morpheus) was used to perform unbiased hierarchical clustering of LATE-NC + samples. Post hoc evaluation of group differences between clusters was performed using a non-parametric Kruskal–Wallis rank sum test, as implemented in R.

Results

Characteristics of the study cohort

The final study sample including $N = 184$ participants. Median age at death among included subjects was 85 years, median Braak NFT stage was III, and approximately one-third of patients were cognitively normal proximal to death. Demographic, clinical, and neuropathologic characteristics of the study cohort are summarized in Table 1. Additional study data are provided in Supplemental Table 1 (online resource).

Clinical, pathologic, and genetic comparisons between LATE-NC + and LATE- participants

Participants with LATE-NC (LATE-NC +) were older at death ($P < 0.0001$) and had a greater level of cognitive impairment ($P < 0.02$) (Table 2). Pathologically, LATE-NC + participants had a higher frequency of HS ($P < 0.00001$). Among amygdala region pathologies, LATE-NC + participants had higher rates of ARTAG ($P < 0.0001$), fibrillary astrocytosis ($P < 0.001$), WM vascular pathology

Table 1 Characteristics of the study sample ($N=184$)

Variable	Frequency/*N*	Median (IQR)/other
Age	–	85 years (11)
Male/female	48% / 52%	85 years (12) / 86 years (10.5)
Cognition[a]		
Dementia	51%	85 years (14)
Mild impairment	15%	89 years (7.5)
Normal	34%	84 years (9)
Brain weight	–	1200 gm (219)
Braak stage	–	NFT stage III (3)
Thal phase	–	Thal Phase 4 (2)
Arteriosclerosis (0–3)[b]	–	1, "Mild" (1)
ADNC level		
High	$N=59$[c]	NFT Stage V ($N=26$), VI ($N=33$)[d]
Intermediate	$N=41$	NFT Stage III ($N=18$), IV ($N=13$), V ($N=10$)
Low	$N=41$	NFT Stage I ($N=15$), II ($N=19$), III ($N=4$), IV ($N=3$)
Not	$N=23$	NFT Stage 0 ($N=3$), I ($N=10$), II ($N=4$), III ($N=4$), IV ($N=2$)
Lewy body pathology		
Transitional/diffuse	18%	NFT stage IV (2.8)
Absent	82%	NFT stage III (3)
Age-related pathology [e]		
PART	18%	–
Argyrophilic grains	28%	–
ARTAG (any)	63%	–
Hippocampal sclerosis		
Present	26%	NFT stage V (2)
Absent	74%	NFT stage III (3)

[a]Cognitive status was unknown in 4 participants, and percentage shown for known samples

[b]For entire brain; see Methods for description

[c]Alzheimer's Disease Neuropathologic Change (ADNC) level for known samples (total *N*)

[d]The number of Braak NFT stages for that ADNC level

[e]For PART, this included "Possible" and "Definite" categories. For ARTAG, this included any form (see text). AGD and ARTAG status were unknown for five participants (% of known samples is shown)

($P<0.05$), and myelin and neuron loss (both $P<0.01$) (Table 2).

LATE-NC + and LATE-NC- participants did not significantly differ in the frequency of Lewy body disease, the frequency of high ADNC, or by NFT stage. The frequency of argyrophilic grains did not significantly differ between groups.

Among SNP genotypes examined, TDP-43 pathology was strongly associated with the presence of a risk allele (A) in *TMEM106B* rs1990622 (OR = 3.3, $P=0.003$) (Table 3).

Patterns of LATE-NC in the amygdala region

As shown in Fig. 2, six key TDP-43 and pTDP morphologies were recorded for each case. It was common that multiple TDP-43 morphologic subtypes were present in a single brain, so individual brains could not be classified by a single feature alone. Therefore, these six morphologies were used in a clustering algorithm, resulting in patterns of LATE-NC that could be discerned in the resulting dendrogram (Fig. 3). These LATE-NC patterns are hereafter referred to as Patterns 1–4. An additional group had a common combination of Patterns 1 and 2 TDP-43 pathologies.

Pattern 1 was distinguished by prominent lamina II TDP-43 pathology in cortical sites of the amygdala region (OTCtx, TECtx, and ECTx), granular preinclusions, and processes in subpial and WM sites. Double labeling with Tau demonstrated these Lamina II inclusions did not co-localize with Tau (see Supplemental Fig. 6a, online resource). In any given microscopic field, the granular preinclusions in Pattern 1 histologically resembled those often seen in ALS and FTLD-TDP patients.

Brains designated as Pattern 2 samples had fibrillary, NFT-like TDP-43 NCIs, corresponding to the previous description of type-β by Josephs and colleagues [27]. These were most conspicuous in TECtx and ECtx. Round NCIs

Table 2 Clinical and pathologic differences between LATE+ and LATE− amygdalae

Variable[a]	LATE+ ($n=107$)	LATE− ($n=77$)	*P* value
Clinical			
Age	88 years (10.5) [b]	83 years (11)	*< 0.0001*
Cognitive impairment	74%	55%	*< 0.02*
Male, female	50% Male, 50% Female	45% Male, 55% Female	NS
Whole brain pathology			
Hippocampal sclerosis	40%	5%	*< 0.00001*
Transitional or diffuse LBD	21%	14%	NS
"High" ADNC	33%	42%	NS
NFT stage	NFT Stage IV (3)	NFT Stage III (3)	NS
Amygdala Region Pathology[c]			
ARTAG	76%	44%	*< 0.0001*
Neuron loss, ECtx (0–3)	1 (2)	1 (1)	*< 0.001*
Myelin loss (LFB) (0–3)	1 (2)	1 (1)	*< 0.01*
Fibrillary astrocytosis (±)	71%	44%	*< 0.001*
Venous collagenosis with rarefied WM (±)	54%	38%	*< 0.05*
Argyrophilic grains	32%	24%	NS

Significant *P*-values are italicized

NS not significant; *ECtx* entorhinal cortex

[a]Determination of LATE+ and LATE− in amygdala region was made blinded to the variables shown in this table (e.g., ARTAG)

[b]Median value (IQR) are shown, unless otherwise specified

[c]Please see Methods for details

Table 3 SNP genotypes of LATE+ and LATE− amygdalae

Gene (SNP ID)	LATE+	LATE−	Odds ratio (CI)	*P* value
TMEM106B (rs1990622)				
Risk allele (A) carrier	90.5%	74.0%	3.3 (1.5–7.9)	*0.003*
APOE (rs429358, rs7412)				
Risk allele (ε4) carrier	36%	42%	0.79 (0.4–1.4)	NS
GRN (rs5848)				
Risk allele (T) carrier	50%	39%	1.6 (0.9–2.9)	NS
ABCC9 (rs704180)				
Risk genotype (AA)	25.5%	24.0%	1.1 (0.5–2.2)	NS
KCNMB2 (rs12496790)				
Risk genotype (AA)	7.8%	3.9%	2.0 (0.5–9.9)	NS

Significant *P*-values are italicized

were variably seen in this pattern, and the junction between ECtx and amygdala (PHA) was a frequent site of involvement. Double labeling studies demonstrated that TDP-43 and Tau co-localized in NCIs of this pattern (see Supplemental Fig. 6b, online resource), as previously described [27].

A common combination of pathologies was seen with features of both Pattern 1 and Pattern 2 in the same brains. These participants had type-β NCIs (NFT-like), as well as small lamina II NCIs and neurites in cortical regions (OTCtx, TECtx, ECtx) (FTLD-like), and NCIs in amygdala. Granular preinclusions were variably seen, as were subpial and WM pTDP-43 immunoreactive processes.

Pattern 3 was characterized by round amygdala pTDP-43 NCIs and thick neurites in amygdala. Brains with this pattern mostly lacked other features of Patterns 1 and 2. pTDP-43 immunoreactive NCIs in Pattern 3 were seen in both CM and BL ROIs and thick neurites were more apparent on pTDP IHC than TDP-43 IHC staining.

Pattern 4 was the most frequent pattern in this study and was represented by subpial and/or WM TDP-43 + processes, often with no or rare NCIs. In these brains there were tortuous subpial TDP-43 + processes often wrapped around corpora amylacea. In WM, they could also be identified adjacent to thick-walled blood vessels, or in rarefied white matter. Double labeling studies demonstrated the TDP-43 processes were bounded by CD44-positive membranes (Supplemental Fig. 7c, online resource). CD44 highlights astrocytic membranes (Supplemental Fig. 7a, online resource), and the TDP-43 processes were in areas enriched for GFAP labeling (not shown), suggesting some component of this pathology is within astrocytes. The TDP-43 + processes did

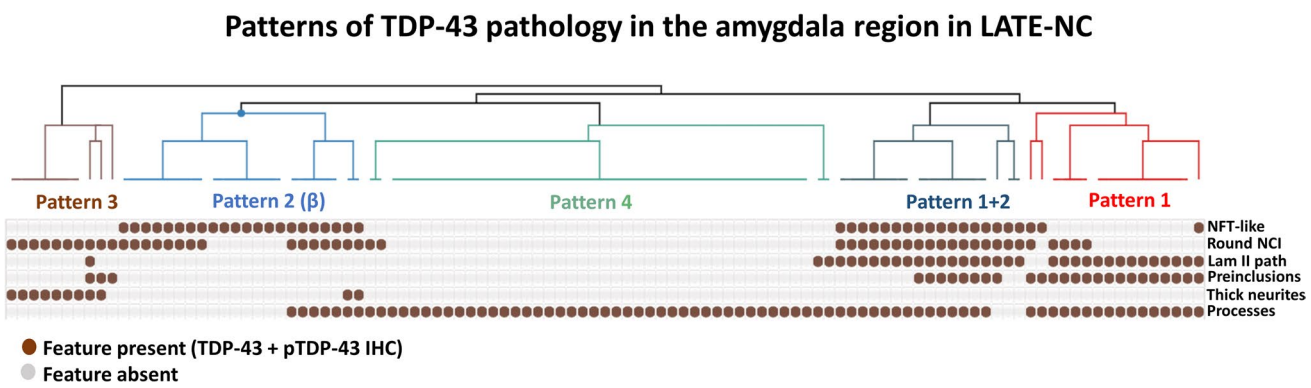

Fig. 3 Patterns of TDP-43 pathology in the amygdala region of patients with LATE-NC ($N = 107$). Unbiased hierarchical clustering was performed in the publicly available program Morpheus (see Methods for detail). The resulting dendrogram is shown, and the TDP-43 morphologies shown to the right ("NFT-like", "Round NCI", etc.) are those illustrated in Fig. 2

not co-localize exactly with tau pathology when ARTAG was also present (Supplemental Fig. 6c, online resource), although both pathologies could affect the same anatomic region. In addition, these TDP-43 + processes did not co-localize with the axonal markers MAP-2, Tubulin, or pan-neuronal marker (Supplemental Fig. 8, online resource).

Comparing parameters between LATE-NC patterns

Table 4 shows how the identified LATE-NC patterns related to other parameters: patient age, LATE-NC stage, Braak NFT stage, ADNC level, presence of LBD, HS, and PART, frequency of the *APOE* ε4 allele, and frequency of normal cognition.

Pattern 1 cases, which may be referred to as "type-α", had the highest frequency of Stage 3 LATE. (The suggested use of type-α here relates to the use of type-α in work of Josephs et al. [27], though here indicating specifically Pattern 1, rather than any non-β TDP-43, as originally described in that work). Despite the superficially FTLD-TDP like lamina II pathology in periallocortical and neocortical regions of amygdala, these patients had one of the highest average ages at death (88 years), being much higher than is typical for FTLD-TDP. In addition, prior work has shown this group typically has less severe pTDP-43 IHC pathology in frontal cortices than is seen in FTLD-TDP [46]. Pattern 1 cases generally had only a limbic Braak NFT stage (III) and > 50% of the cases had "No" or "Low" ADNC. The *APOE* ε4 allele was not enriched in this group.

Pattern 2, which we designated "type-β" for consistency with Josephs et al. [27], had the highest levels of ADNC including highest median NFT stage. This group was enriched for the *APOE* ε4 allele (> 60%). In distinction from Pattern 1, this group had more frequent LATE-NC Stage 1, and especially LATE-NC Stage 2 cases.

The combination Pattern 1 + 2 group had a similar profile to Pattern 2, with higher ADNC and higher NFT stage, and was similarly enriched for Stage 2 LATE-NC and *APOE* ε4 (like Pattern 2 samples). Features of Pattern 1 were also present, including lamina II pTDP-43 NCIs. The rates of cognitive impairment (100%) and comorbid HS (82%) were greatest in this group.

Pattern 3 generally lacked features of Patterns 1 and 2, and instead had rounded amygdala NCIs. This pattern was most notable for the high frequency of transitional and diffuse LBD (60%) as compared to other pTDP-43 pathologic patterns (Table 4). Pattern 3 brains were predominantly LATE-NC Stage 1. Nonetheless, among persons with Pattern 3 samples, all had cognitive impairment.

Pattern 4 was the most prevalent LATE-NC group, constituting nearly 40% of all LATE-NC + samples in this study. Most participants with Pattern 4 were LATE-NC Stage 1. Further, normal cognition was most common in this group, and HS co-pathology was least common. This group had the lowest median NFT stage and the most frequent "No" or "Low" ADNC levels, as well as the highest rate of comorbid PART pathology. Building on the earlier use of "type α" and "type β" by Josephs and colleagues [27], we suggest the use of "type γ" and "type δ" for Patterns 3 and 4, respectively (see Table 4).

Distribution of pTDP pathology in early and advanced LATE-NC stages

Figure 4 shows a heatmap depicting the regional variation in pTDP-43 pathology, independent of morphologic type. In this heatmap, each ROI is a column (e.g., "white matter beneath amygdala"), each unique participant is a row, and samples are arranged by three LATE-NC stages (see labels at left). Within each LATE-NC stage, rows are arranged by the overall pathologic severity in the sample, such that the

Table 4 Patterns of LATE-NC in the amygdala region based on hierarchical clustering

Pattern	Symbol[a]	TDP-43	Age	Frequency	Stage 1	Stage 2	Stage 3	NFT stage	No/Low ADNC	LBD[c]	PART[d]	Hipp Scl	APOE ε4	Normal cognition
1	α	Lamina II NCIs + short neurites, many granular preinclusions[b]	87.9	15%	13%	50%	**38%**	III	**63%**	6%	20%	**56%**	25%	38%
2	β	NFT-like NCIs, no/rare preinclusions	86.4	21%	**29%**	**67%**	5%	**V**	14%	27%	5%	**55%**	**64%**	18%
1 + 2	β + α	Features of Patterns 1 and 2	88.5	16%	**6%**	**76%**	18%	IV–V	18%	24%	0%	**82%**	50%	0%
3	γ	Round NCIs in amygdala + thick neurites	76.8	9%	**78%**	**11%**	11%	IV	20%	**60%**	0%	20%	50%	0%
4	δ	Subpial and WM processes, no/rare NCIs	86.2	39%	**62%**	**33%**	5%	**II**	**62%**	14%	**25%**	14%	17%	**44%**
		P value [e]	-	–	–	–	*< 0.001*	*< 0.001*	*< 0.0002*	*0.01*	*0.05*	*< 0.001*	*< 0.002*	*< 0.002*

Notable values for the Patterns shown are indicated in bold type

NS not significant

[a]Proposed terminology (see Discussion)

[b]Granular preinclusions with loss of nuclear staining and accumulated cytoplasmic TDP-43, as seen in ALS and FTLD-TDP, using non-phosphorylated TDP-43

[c]Transitional and diffuse Lewy body disease

[d]Including both "Possible" and "Definite" PART

[e]*P* value from non-parametric ANOVA (Kruskal–Wallis rank sum test) of these variables, with cluster as the grouping variable. *TMEM106B* and *GRN* risk allele frequency did not significantly vary across clusters (data not shown)

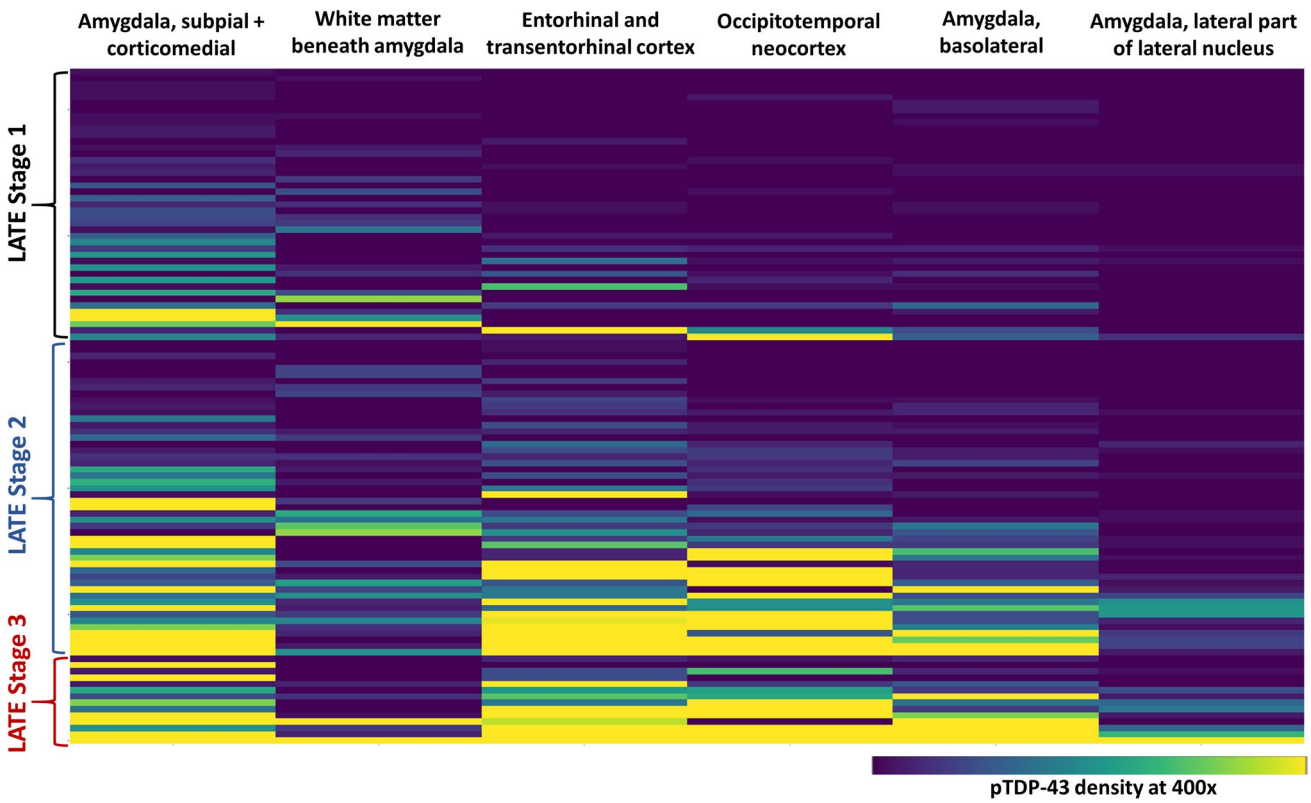

Fig. 4 LATE-NC ordered by pTDP-43 severity and grouped by LATE-NC stage. This heat map shows the regional distribution of pTDP-43 pathology in six study ROIs in all subjects with LATE-NC, independent of inclusion morphology. Samples are grouped by LATE-NC stage 1 (top), stage 2 (middle) and stage 3 (bottom). Ordering of cases within each stage is based on the average pTDP-43 inclusion density across the ROIs, ordered from low to high. The density of pTDP-43 inclusion pathology is indicated by the bar at the bottom right of the heat map

top rows within "LATE Stage 1" and "LATE Stage 2" are the samples with the mildest pTDP-43 pathology within that group.

In LATE-NC Stages 1 and 2, the ROIs with the earliest and mildest pathology were CM amygdala, WM, and ECtx/TECtx (Fig. 4). As TDP-43 pathologic burden increased within stages 1 and 2 LATE-NC, not only did CM, WM and ECtx/TECtx become more severely involved, but OTCtx and BL amygdala also became more involved. In contrast, the La-L region was rarely involved outside of more severe Stage 2 and Stage 3 samples. Thus, both within and across LATE-NC Stages, a pattern of medial to lateral and ventrolateral to dorsolateral anatomic involvement by TDP-43 pathology was seen.

As shown in Supplemental Fig. 9, there were additional regions with infrequent pTDP pathology. These included not only La-L, but also WM of the inferior longitudinal fasciculus (lateral to La-L), ventral extension of claustrum (lateral to La-L), the centromedian nuclear complex of the amygdala (abutting the entorhinal fissure), and the magnocellular neurons of basal forebrain.

Discussion

This study builds on prior work to generate insights into the heterogeneity and evolution of LATE-NC in aged brains. As in earlier studies, LATE-NC was associated with HS, older age, cognitive impairment, and the *TMEM106B* risk genotype. Among amygdala region pathologies, LATE-NC was associated with myelin loss, entorhinal cortex cell dropout, astrocytosis, and white matter vascular pathology, as well as amygdala region ARTAG. Using a clustering algorithm, we found four different patterns of LATE-NC pathology, sometimes apparently initiated outside the "amygdala proper", but within the amygdala region. Although TDP-43 pathologies converged on common anatomic foci at higher stages, the patterns identified were clinically, pathologically, and genetically differentiable. One of these patterns (Pattern 4, or δ) was commonly seen in persons dying without documented cognitive impairment, and in isolation may represent a subclinical pathology.

Methodological strengths of the study included that LATE-NC pathology was determined blinded to other pathologic, clinical, and genetic data. Participants included both

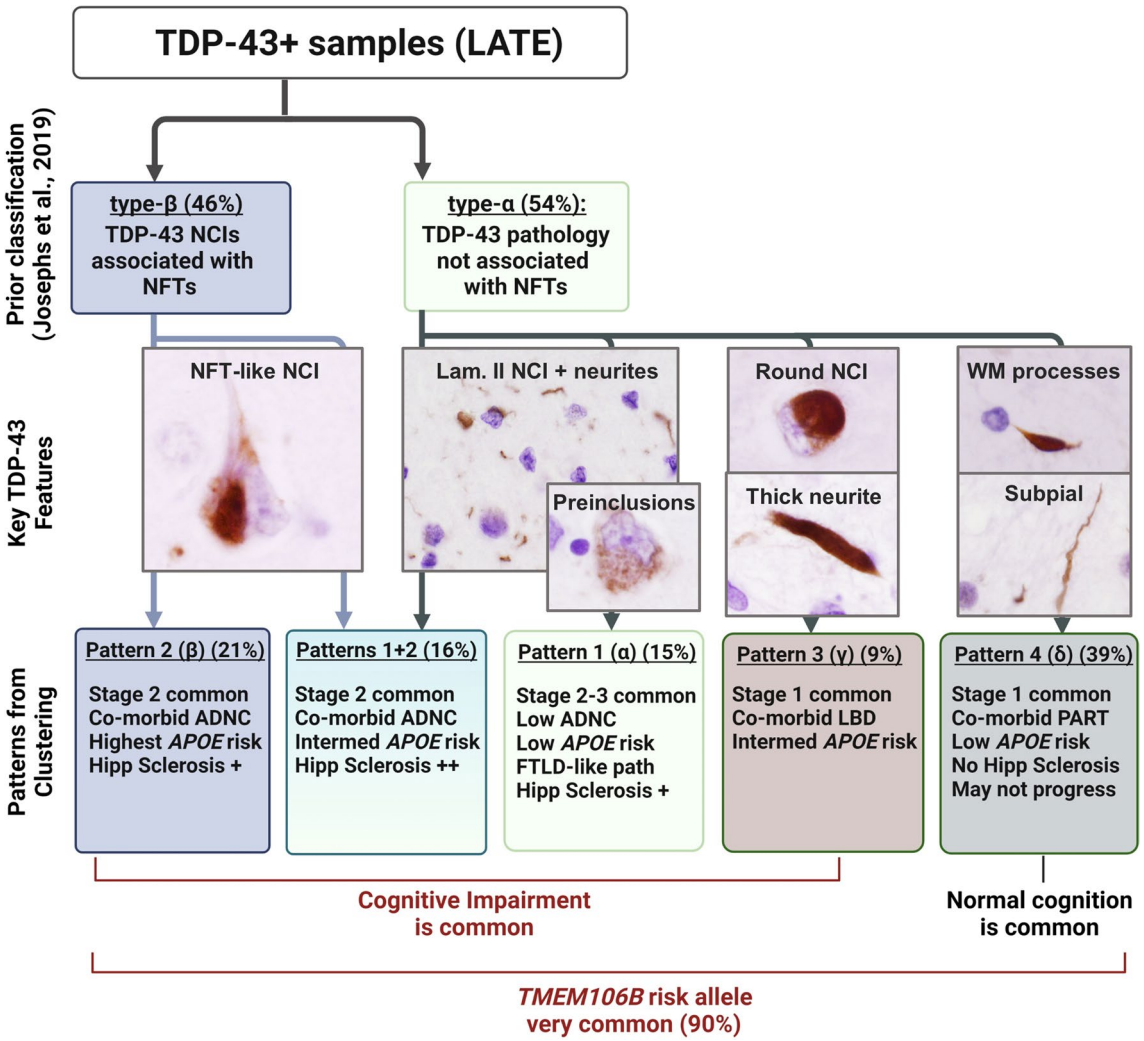

Fig. 5 A proposed classification scheme for LATE-NC. Hierarchical clustering identified four patterns of LATE-NC (Patterns 1–4), and one group with combined features of Patterns 1 + 2, and the salient pathologic and clinical features are shown in this schematic. Consistent with the earlier work of Josephs et al. (2019), type-β is applied to the cluster-derived Pattern 2 (β). Also as in that earlier study, type-α refers to non-NFT associated TDP-43 pathology, but only to the FTLD-like lamina II pathology with frequent preinclusions (Pattern 1, or α). Schematic created (in part) with BioRender

TDP-43-negative samples and many brains in early stages of LATE-NC. The TDP-43 pathologic patterns were also determined using relatively unbiased clustering methods, and we correlated the pathologic findings with a large variety of additional clinical and neuropathologic data. Both phosphorylated and non-phosphorylated TDP-43 antibodies were used on serially sectioned brain portions, with the determination that either staining approach is suitable for the neuropathological evaluation of LATE-NC.

Earlier studies of TDP-43 pathology have identified stage 1 pathology within amygdala [28, 39, 42], with stage 2 being in hippocampus and higher stages involving neocortex, as well as subcortical structures. Notably, the "amygdala" is not a single structure, but rather a complex collection of disparate cell groups, bounded by disparate structures such as entorhinal cortex, basal forebrain, white matter tracts, and anterior hippocampus [2, 4, 33, 54]. When only one brain region was involved in the mildest forms of LATE-NC, the affected anatomical focus was often outside of the amygdala proper (e.g., subpial CM, white matter, or periallocortex). We, therefore, propose that the stage 1 of LATE-NC be referred to as "amygdala region", rather than "amygdala". This will harmonize the diagnostic criteria with observed phenomena and should increase the sensitivity of neuropathologic evaluation to detecting early LATE-NC. "Amygdala region" (LATE stage 1) would include cases with TDP-43 pathology limited to periallocortex (transentorhinal, entorhinal cortex), non-gray matter structures (subpial region overlying amygdala, white matter beneath amygdala), and even the anterior portion of hippocampus that

abuts amygdala, often sampled in more caudal or obliquely oriented sections through amygdala. We note that just as LATE-NC stage 1 may be subclinical [42], there are analogous stages of other early pathologies (e.g., Braak NFT stages I–III, Thal Aβ phases 1–2) that also are often seen in cognitively normal persons [25, 45].

A primary finding in the present study was that there were four patterns of LATE-NC, based on the clustering of 6 common types of TDP-43 pathologies. These patterns broadly replicate and extend an earlier landmark study, which identified two distinct patterns of LATE-NC, termed type-α and type-β [27]. A new proposed terminology reconciles both the prior work and the current study (Table 4), and this is further illustrated in the schematic of Fig. 5.

Analogous to the prior study by Josephs et al. [27], Pattern 1 (comparable to type α) refers specifically to those cases with FTLD-like lamina II pathology in periallocortical (TECtx, ECtx) and neocortical regions (OTCtx) of a section through amygdala. We also found that these cases have frequent granular preinclusions, readily detected by non-phosphorylated TDP-43 IHC, which may help to confirm the presence of this pattern in addition to its other features. Pattern 1 (type α) was associated with higher LATE-NC stages and non-NFT pathology. Pattern 2 (type β) with NFT-like TDP-43 NCIs was associated with tau-immunoreactive NFT pathology and lower LATE-NC stage. A difference from the prior study [27], which designated cases as either being type α or type β patterns, is that we also identified brains with coexisting features of both Pattern 1 (type-α) and Pattern 2 (type-β). This observation was previously described in a separate study wherein multiple neuropathologists assessed each case blindly [46]. Additional work is needed to determine whether the co-occurrence of TDP-43 morphologies in Pattern 1 + 2 cases is coincidental, or whether the different TDP-43 pathologies are synergistic with each other.

All TDP-43 pathologies studied here were identified using both phospho-TDP-43 and non-phospho-TDP-43 antibodies. The use of both antibodies is not required, although pTDP IHC was more sensitive to certain inclusion types (e.g., NFT-like, or type-β). Conversely, the non-phospho-TDP-43 antibody demonstrates both loss of nuclear labeling and early granular cytoplasmic inclusion pathology, and was more sensitive to granular preinclusions, as previously reported in ALS/FTLD-TDP spectrum brains [10, 13, 17]. Of note, granular preinclusions did not appear in all forms of advanced TDP-43 proteinopathy, and extensive Pattern 2 (type β) pathology with no granular preinclusion pathology could often be identified. In contrast, granular preinclusion pathology was a consistent feature in Pattern 1 (type-α) samples. The molecular factors contributing to this morphology deserve further investigation.

Brains with LATE-NC significantly differed from those without LATE-NC in several ways that were previously described, including increased frequencies of cognitive impairment [53] and comorbid HS [3, 26]. LATE-NC + samples also had more amygdala region ARTAG and myelin loss. Further, LATE-NC in all its forms was associated with the presence of a *TMEM106B* risk allele. This finding replicates earlier studies reporting an association between *TMEM106B* and LATE/HS-Aging [19, 27, 43]. The strong association between LATE-NC and *TMEM106B* in this study is notable provided the modest sample size, the widely varying severity and patterns of TDP-43 proteinopathy, and the inclusion of cognitively normal participants; thus, the *TMEM106B* risk allele is a key risk factor for LATE-NC across all patterns of pathology. Although the *APOE* risk allele did not necessarily associate with LATE-NC in Patterns 1 and 4, *APOE* ε4 was enriched in samples with prominent type-β NCI pathology (Pattern 2), and in samples with Pattern 3 (type γ).

Two novel patterns described here are proposed as Pattern 3 (type γ) and Pattern 4 (type δ). Pattern 3 samples had round NCIs and thick neurites in amygdala, usually without other forms of LATE-NC pathology. Pattern 3 was always associated with cognitive impairment and had the highest rate of transitional and diffuse LBD. Others have found that LATE-NC may have a unique phenotype in patients with LBD [1, 5, 52]. Although enriched in these cases, transitional and diffuse LBD was not exclusive to Pattern 3 (see Table 4), and other TDP-43 morphologies may emerge in higher LATE-NC stages in the setting of LBD.

Pattern 4 (type δ) was the most subtle subtype of LATE-NC, featuring TDP-43 + processes in subpial amygdala and/or subamygdaloid WM, often in the absence of NCI pathology. This corresponds to a morphology of TDP-43 first reported in detail by Arnold and colleagues [6], who also reported a similar anatomic distribution. While these TDP-43 immunoreactive structures may resemble neurites [34], in this study we demonstrate that these TDP-43 + processes were present in cells that were immunoreactive for CD44 (see Supplemental Fig. 7, online resource). CD44 is a glycoprotein expressed on the surface of the cell body and processes of astrocytes [21, 38]. By contrast, the TDP-43 + processes did not co-localize with three axonal markers. This suggests that the processes in Pattern 4 may be, at least in part, arising within astrocytes. The close association of Pattern 4 LATE-NC with corpora amylacea is also consistent with this interpretation.

Participants with Pattern 4 pathology in isolation had the lowest rates of ADNC and HS, and the lowest frequency of *APOE* ε4. Most Pattern 4 cases were LATE-NC Stage 1, and nearly half of the group was cognitively normal. Since some Pattern 4 cases were cognitively impaired, the pathological diagnosis is likely still warranted with the expectation that LATE-NC stage 1 may often be subclinical. However, our cross-sectional data, including many

Pattern 4 cases with LATE-NC stage 1, raise the question as to whether some brains with Pattern 4 TDP-43 pathology in isolation will not progress further in terms of pathologic severity, perhaps analogous to how PART-may not progress to neocortical Braak NFT stages even in very advanced age [14]. An alternative hypothesis is that some Pattern 4 brains would have developed more pathology if they had progressed in age. One finding that suggests Pattern 4 may be more than a coincidental pathology is that these cases had an elevated frequency of the *TMEM106B* risk allele (90.5%), compared to samples without LATE-NC (74%). This does suggest a common pathogenetic pathway in the different LATE-NC subtypes, even with very mild pathology, and suggests that there may be compensatory mechanisms in some Pattern 4 cases. To test these hypotheses will require future studies.

There are limitations to the current work. The sample size was modest with a total of 184 cases studied. In addition, among study participants, the *APOE* risk allele rate (38.2% of study samples) indicated that there was a recruitment bias with a tendency for study samples to have higher-than-normal risk for developing ADNC. Other aspects of potential bias include the general tendency for brain banks to be enriched for high-socioeconomic status patients who may die at older ages than the general population and thus have elevated dementia risk. For definitive establishment of associations between LATE-NC patterns and clinical features, more work will be required. Future studies in larger cohorts, including more diverse samples from additional centers, are needed. An additional area not examined here and requiring further study is whether specific clinical syndromes were associated with LATE-NC patterns, or specific anatomic sites of involvement e.g., selective memory impairment, anomia, other language impairments, and/or prosopagnosia.

In summary, early foci of LATE-NC TDP-43 pathology occurred at several anatomic locations in the "amygdala region" and not only within the amygdala proper. Certain parameters and features, e.g., *APOE* risk alleles, HS, higher NFT stages, Lewy body pathology, and clinical impairment severity were associated with given patterns of LATE-NC. However, the *TMEM106B* risk allele was elevated in all LATE-NC patterns, which is remarkable given the heterogeneity of the TDP-43 pathology identified. The different TDP-43 patterns also tended to converge in the more severely affected brains, and each pattern could be seen at any given LATE-NC stage. Thus, our findings support the idea that there are meaningful commonalities under the umbrella diagnosis of LATE-NC.

Supplementary Information The online version contains supplementary material available at https://doi.org/10.1007/s00401-022-02416-5.

Acknowledgements We are grateful to the study participants and families who made this research possible. We appreciate the excellent technical work provided by the personnel of the autopsy and laboratory divisions in the Department of Pathology and Genomic Medicine at Houston Methodist and the University of Kentucky Alzheimer's Disease Research Center. We thank Dr. Dennis Dickson (Mayo Clinic, Jacksonville, Florida), who suggested the use of CD44 staining for process predominant cases in Pattern 4.

Funding Work was supported by a Clinician-Scientist Research Award from the Institute of Academic Medicine at the Houston Methodist Research Institute, an Investigator-initiated Research Award from the ALS Association (ALSA), and NIH/NINDS (RF1NS118584). The University of Kentucky Alzheimer's Disease Research Center is supported by NIH/NIA P30AG072946. Additional support provided by NIH/NIA (R01 AG061111) and NIH/NIA (R01 AG057187).

Data availability statement Data and/or supporting microscopic images from this study are available from the corresponding author upon reasonable request.

Declarations

Conflict of interest The authors report no competing interests.

References

1. Agrawal S, Yu L, Nag S, Arfanakis K, Barnes LL, Bennett DA et al (2021) The association of Lewy bodies with limbic-predominant age-related TDP-43 encephalopathy neuropathologic changes and their role in cognition and Alzheimer's dementia in older persons. Acta Neuropathol Commun 9:156. https://doi.org/10.1186/s40478-021-01260-0
2. Alheid GF, de Olmos JS, Beltramino CA (1995) Amygdala and extended amygdala. In: Paxinos G (ed) The rat nervous system, 2nd edn. Academic Press, London, pp 495–578
3. Amador-Ortiz C, Lin WL, Ahmed Z, Personett D, Davies P, Duara R et al (2007) TDP-43 immunoreactivity in hippocampal sclerosis and Alzheimer's disease. Ann Neurol 61:435–445. https://doi.org/10.1002/ana.21154
4. Amunts K, Kedo O, Kindler M, Pieperhoff P, Mohlberg H, Shah NJ et al (2005) Cytoarchitectonic mapping of the human amygdala, hippocampal region and entorhinal cortex: intersubject variability and probability maps. Anat Embryol (Berl) 210:343–352. https://doi.org/10.1007/s00429-005-0025-5
5. Aoki N, Murray ME, Ogaki K, Fujioka S, Rutherford NJ, Rademakers R et al (2015) Hippocampal sclerosis in Lewy body disease is a TDP-43 proteinopathy similar to FTLD-TDP

Type A. Acta Neuropathol 129:53–64. https://doi.org/10.1007/s00401-014-1358-z
6. Arnold SJ, Dugger BN, Beach TG (2013) TDP-43 deposition in prospectively followed, cognitively normal elderly individuals: correlation with argyrophilic grains but not other concomitant pathologies. Acta Neuropathol 126:51–57. https://doi.org/10.1007/s00401-013-1110-0
7. Braak H (1980) Architectonics of the human telencephalic cortex. Springer-Verlag, Berlin
8. Braak H, Braak E (1987) Argyrophilic grains: characteristic pathology of cerebral cortex in cases of adult onset dementia without Alzheimer changes. Neurosci Lett 76:124–127. https://doi.org/10.1016/0304-3940(87)90204-7
9. Braak H, Braak E (1991) Neuropathological stageing of Alzheimer-related changes. Acta Neuropathol 82:239–259
10. Brandmeir NJ, Geser F, Kwong LK, Zimmerman E, Qian J, Lee VM et al (2008) Severe subcortical TDP-43 pathology in sporadic frontotemporal lobar degeneration with motor neuron disease. Acta Neuropathol 115:123–131. https://doi.org/10.1007/s00401-007-0315-5
11. Brenowitz WD, Monsell SE, Schmitt FA, Kukull WA, Nelson PT (2014) Hippocampal sclerosis of aging is a key Alzheimer's disease mimic: clinical-pathologic correlations and comparisons with both Alzheimer's disease and non-tauopathic frontotemporal lobar degeneration. J Alzheimers Dis 39:691–702
12. Cairns NJ, Neumann M, Bigio EH, Holm IE, Troost D, Hatanpaa KJ et al (2007) TDP-43 in familial and sporadic frontotemporal lobar degeneration with ubiquitin inclusions. Am J Pathol 171:227–240
13. Cathcart SJ, Appel SH, Peterson LE, Greene EP, Powell SZ, Arumanayagam AS et al (2021) Fast progression in amyotrophic lateral sclerosis is associated with greater TDP-43 burden in spinal cord. J Neuropathol Exp Neurol. https://doi.org/10.1093/jnen/nlab061
14. Crary JF, Trojanowski JQ, Schneider JA, Abisambra JF, Abner EL, Alafuzoff I et al (2014) Primary age-related tauopathy (PART): a common pathology associated with human aging. Acta Neuropathol 128:755–766. https://doi.org/10.1007/s00401-014-1349-0
15. Crosby EC, Humphrey T, Lauer EW (1962) Correlative anatomy of the nervous system. MacMillan, New Jersey
16. Cykowski MD, Dickson DW, Powell SZ, Arumanayagam AS, Rivera AL, Appel SH (2019) Dipeptide repeat (DPR) pathology in the skeletal muscle of ALS patients with C9ORF72 repeat expansion. Acta Neuropathol 138:667–670. https://doi.org/10.1007/s00401-019-02050-8
17. Cykowski MD, Powell SZ, Peterson LE, Appel JW, Rivera AL, Takei H et al (2017) Clinical significance of TDP-43 neuropathology in amyotrophic lateral sclerosis. J Neuropathol Exp Neurol 76:402–413. https://doi.org/10.1093/jnen/nlx025
18. Cykowski MD, Takei H, Schulz PE, Appel SH, Powell SZ (2014) TDP-43 pathology in the basal forebrain and hypothalamus of patients with amyotrophic lateral sclerosis. Acta Neuropathol Commun 2:171. https://doi.org/10.1186/s40478-014-0171-1
19. Dugan AJ, Nelson PT, Katsumata Y, Shade LMP, Boehme KL, Teylan MA et al (2021) Analysis of genes (TMEM106B, GRN, ABCC9, KCNMB2, and APOE) implicated in risk for LATE-NC and hippocampal sclerosis provides pathogenetic insights: a retrospective genetic association study. Acta Neuropathol Commun 9:152. https://doi.org/10.1186/s40478-021-01250-2
20. Economo C, Triarhou LC (2009) Cellular structure of the human cerebral cortex. Karger, Berlin
21. Feany MB, Dickson DW (1995) Widespread cytoskeletal pathology characterizes corticobasal degeneration. Am J Pathol 146:1388–1396
22. Gilbert AR, Chevez-Barrios P, Cykowski MD (2018) Perineurial-like cells and EMA expression in the suprachoroidal region of the human Eye. J Histochem Cytochem 66:367–375. https://doi.org/10.1369/0022155418756308
23. Hu WT, Josephs KA, Knopman DS, Boeve BF, Dickson DW, Petersen RC et al (2008) Temporal lobar predominance of TDP-43 neuronal cytoplasmic inclusions in Alzheimer disease. Acta Neuropathol 116:215–220. https://doi.org/10.1007/s00401-008-0400-4
24. James BD, Wilson RS, Boyle PA, Trojanowski JQ, Bennett DA, Schneider JA (2016) TDP-43 stage, mixed pathologies, and clinical Alzheimer's-type dementia. Brain 139:2983–2993. https://doi.org/10.1093/brain/aww224
25. Jicha GA, Abner EL, Schmitt FA, Kryscio RJ, Riley KP, Cooper GE et al (2012) Preclinical AD workgroup staging: pathological correlates and potential challenges. Neurobiol Aging 33:622 e621-622 e616. https://doi.org/10.1016/j.neurobiolaging.2011.02.018
26. Jicha GA, Nelson PT (2019) Hippocampal sclerosis, argyrophilic grain disease, and primary age-related tauopathy. Continuum (Minneap Minn) 25:208–233. https://doi.org/10.1212/CON.0000000000000697
27. Josephs KA, Murray ME, Tosakulwong N, Weigand SD, Serie AM, Perkerson RB et al (2019) Pathological, imaging and genetic characteristics support the existence of distinct TDP-43 types in non-FTLD brains. Acta Neuropathol 137:227–238. https://doi.org/10.1007/s00401-018-1951-7
28. Josephs KA, Murray ME, Whitwell JL, Tosakulwong N, Weigand SD, Petrucelli L et al (2016) Updated TDP-43 in Alzheimer's disease staging scheme. Acta Neuropathol 131:571–585. https://doi.org/10.1007/s00401-016-1537-1
29. Josephs KA, Whitwell JL, Knopman DS, Hu WT, Stroh DA, Baker M et al (2008) Abnormal TDP-43 immunoreactivity in AD modifies clinicopathologic and radiologic phenotype. Neurology 70:1850–1857. https://doi.org/10.1212/01.wnl.0000304041.09418.b1
30. Katsumata Y, Fardo DW, Kukull WA, Nelson PT (2018) Dichotomous scoring of TDP-43 proteinopathy from specific brain regions in 27 academic research centers: associations with Alzheimer's disease and cerebrovascular disease pathologies. Acta Neuropathol Commun 6:142. https://doi.org/10.1186/s40478-018-0641-y
31. Kovacs GG, Ferrer I, Grinberg LT, Alafuzoff I, Attems J, Budka H et al (2016) Aging-related tau astrogliopathy (ARTAG): harmonized evaluation strategy. Acta Neuropathol 131:87–102. https://doi.org/10.1007/s00401-015-1509-x
32. Kovacs GG, Robinson JL, Xie SX, Lee EB, Grossman M, Wolk DA et al (2017) Evaluating the patterns of aging-related tau astrogliopathy unravels novel insights into brain aging and neurodegenerative diseases. J Neuropathol Exp Neurol 76:270–288. https://doi.org/10.1093/jnen/nlx007
33. LeDoux J (2007) The amygdala. Curr Biol 17:R868-874. https://doi.org/10.1016/j.cub.2007.08.005
34. Mackenzie IR, Bigio EH, Ince PG, Geser F, Neumann M, Cairns NJ et al (2007) Pathological TDP-43 distinguishes sporadic amyotrophic lateral sclerosis from amyotrophic lateral sclerosis with SOD1 mutations. Ann Neurol 61:427–434. https://doi.org/10.1002/ana.21147
35. Mai J, Majtanik M, Paxinos G (2016) Atlas of the human brain. Elsevier, Amsterdam
36. Mirra SS, Heyman A, McKeel D, Sumi SM, Crain BJ, Brownlee LM et al (1991) The Consortium to Establish a Registry for Alzheimer's Disease (CERAD). Part II. Standardization of the neuropathologic assessment of Alzheimer's disease. Neurology 41:479–486. https://doi.org/10.1212/wnl.41.4.479
37. Montine TJ, Phelps CH, Beach TG, Bigio EH, Cairns NJ, Dickson DW et al (2012) National Institute on Aging-Alzheimer's Association guidelines for the neuropathologic assessment of Alzheimer's

disease: a practical approach. Acta Neuropathol 123:1–11. https://doi.org/10.1007/s00401-011-0910-3
38. Moretto G, Xu RY, Kim SU (1993) CD44 expression in human astrocytes and oligodendrocytes in culture. J Neuropathol Exp Neurol 52:419–423. https://doi.org/10.1097/00005072-199307000-00009
39. Nag S, Yu L, Boyle PA, Leurgans SE, Bennett DA, Schneider JA (2018) TDP-43 pathology in anterior temporal pole cortex in aging and Alzheimer's disease. Acta Neuropathol Commun 6:33. https://doi.org/10.1186/s40478-018-0531-3
40. Nelson PT, Abner E, Patel E, Anderson S, Wilcock DM, Kryscio RJ et al (2018) The amygdala as a locus of pathologic misfolding in neurodegenerative diseases. J Neuropathol Exp Neurol 77:2–20
41. Nelson PT, Abner EL, Schmitt FA, Kryscio RJ, Jicha GA, Smith CD et al (2008) Modeling the association between 43 different clinical and pathological variables and the severity of cognitive impairment in a large autopsy cohort of elderly persons. Brain Pathol 20:66–79
42. Nelson PT, Dickson DW, Trojanowski JQ, Jack CR, Boyle PA, Arfanakis K et al (2019) Limbic-predominant age-related TDP-43 encephalopathy (LATE): consensus working group report. Brain 142:1503–1527. https://doi.org/10.1093/brain/awz099
43. Nelson PT, Gal Z, Wang WX, Niedowicz DM, Artiushin SC, Wycoff S et al (2019) TDP-43 proteinopathy in aging: Associations with risk-associated gene variants and with brain parenchymal thyroid hormone levels. Neurobiol Dis 125:67–76. https://doi.org/10.1016/j.nbd.2019.01.013
44. Neumann M, Sampathu DM, Kwong LK, Truax AC, Micsenyi MC, Chou TT et al (2006) Ubiquitinated TDP-43 in frontotemporal lobar degeneration and amyotrophic lateral sclerosis. Science 314:130–133
45. RijalUpadhaya A, Kosterin I, Kumar S, von Arnim CA, Yamaguchi H, Fandrich M et al (2014) Biochemical stages of amyloid-beta peptide aggregation and accumulation in the human brain and their association with symptomatic and pathologically preclinical Alzheimer's disease. Brain 137:887–903. https://doi.org/10.1093/brain/awt362
46. Robinson JL, Porta S, Garrett FG, Zhang P, Xie SX, Suh E et al (2020) Limbic-predominant age-related TDP-43 encephalopathy differs from frontotemporal lobar degeneration. Brain 143:2844–2857. https://doi.org/10.1093/brain/awaa219
47. Schmitt FA, Nelson PT, Abner E, Scheff S, Jicha GA, Smith C et al (2012) University of Kentucky Sanders-Brown healthy brain aging volunteers: donor characteristics, procedures and neuropathology. Curr Alzheimer Res 9:724–733. https://doi.org/10.2174/156720512801322591
48. Swanson LW, Petrovich GD (1998) What is the amygdala? Trends Neurosci 21:323–331
49. R Core Team (2021) R: a language and environment for statistical computing. R Foundation for Statistical Computing, Vienna, Austria. https://www.R-project.org/
50. Thal DR, Rub U, Orantes M, Braak H (2002) Phases of A beta-deposition in the human brain and its relevance for the development of AD. Neurology 58:1791–1800
51. Uchino A, Takao M, Hatsuta H, Sumikura H, Nakano Y, Nogami A et al (2015) Incidence and extent of TDP-43 accumulation in aging human brain. Acta Neuropathol Commun 3:35. https://doi.org/10.1186/s40478-015-0215-1
52. Uemura MT, Robinson JL, Cousins KAQ, Tropea TF, Kargilis DC, McBride JD et al (2022) Distinct characteristics of limbic-predominant age-related TDP-43 encephalopathy in Lewy body disease. Acta Neuropathol 143:15–31. https://doi.org/10.1007/s00401-021-02383-3
53. Wilson RS, Yu L, Trojanowski JQ, Chen EY, Boyle PA, Bennett DA et al (2013) TDP-43 pathology, cognitive decline, and dementia in old age. JAMA Neurol 70:1418–1424. https://doi.org/10.1001/jamaneurol.2013.3961
54. Yilmazer-Hanke D (2012) Amygdala. In: Mai J, Paxinos G (eds) The human nervous system, 3rd edn. Elsevier, Amsterdam, pp 759–835